Photonics and Nanostructures – Fundamentals and Applications 29 (2018) 30–35

Contents lists available at ScienceDirect

Photonics and Nanostructures – Fundamentals and Applications

journal homepage: www.elsevier.com/locate/photonics

Invited Paper

Optimal configuration of partial Mueller matrix polarimeter for measuring the ellipsometric parameters in the presence of Poisson shot noise and Gaussian noise

Naicheng Quan [a,*], Chunmin Zhang [b], Tingkui Mu [b]

[a] School of materials science and Engineering, Xi'an University of technology, Xi'an, 710048, China
[b] Institute of Space optics, Xi'an Jiaotong University, Xi'an, 710049, China

ARTICLE INFO

Article history:
Received 30 November 2017
Received in revised form 1 January 2018
Accepted 19 January 2018
Available online 3 February 2018

Keywords:
Polarimetry
Mueller matrix
Ellipsometric parameters

ABSTRACT

We address the optimal configuration of a partial Mueller matrix polarimeter used to determine the ellipsometric parameters in the presence of additive Gaussian noise and signal-dependent shot noise. The numerical results show that, for the PSG/PSA consisting of a variable retarder and a fixed polarizer, the detection process immune to these two types of noise can be optimally composed by 121.2° retardation with a pair of azimuths ±71.34° and a 144.48° retardation with a pair of azimuths ±31.56° for four Mueller matrix elements measurement. Compared with the existing configurations, the configuration presented in this paper can effectively decrease the measurement variance and thus statistically improve the measurement precision of the ellipsometric parameters.

1. Introduction

Mueller matrix polarimeter (MMP) can measure all the 16 elements of Mueller matrix of the sample that provide the parameters related to optical properties. As such, MMP has widely used in accurate determination of dielectric function, optical properties and geometric characteristics of thin films [1–8]. A typical MMP consists of a complete polarization state generator (PSG) and a polarization state analyzer (PSA), which can determine the polarization altering properties of a sample both in reflection and in transmission. A PSA/PSG generally consists of a polarizer and an active birefringent optical component either modulated by azimuthal rotation or by an externally applied electric field, such as rotating (waveplate/bi-prism) retarders, electro-optical modulation, photoelastic modulators, and liquid crystal retarders [9–13].

The practical detection process invariably has noises that disturb the measurement and reduce the accuracy of the reconstructed Mueller matrix. Two types of noise are frequently encountered and considered statistically: Gaussian additive noise, representative of sensor noise, and Poisson shot noise that results from the quantum fluctuations of the useful or ambient light flux [14–16]. In the design of MMP, optimizing the instrument matrices of PSG and PSA is an effective way to minimize the estimation variance. The retardations and azimuths of retarders relative to instrument matrices are optimized by using the specified metrics such as condition number (CN) or equally weighted variance (EWV) [17–26]. However, the noise variances in the measured Mueller matrix for such optimized MMPs are still sensitive to the Poisson noise. Anna et al. optimized the instrument matrices by minimizing total variance of all the 16 elements in the measured Mueller matrix for both Gaussian noise and Poisson noise and demonstrated an ideal instrument matrix model [15]. The MMP corresponds to such ideal instrument matrix is insensitive to both Gaussian additive noise and Poisson shot noise. Mu et al. proposed a method that minimizing the Euclidean distance between the practical instrument matrices and the ideal one for determining the optimum configuration of Full-Stokes polarimeter architecture with the immunity to both Poisson and Gaussian noise, which can be also used to determine the optimum configuration of PSG/PSA in MMP [27]. Under certain circumstances, some elements in the Mueller matrix of anisotropic optical materials are zeros that makes the Mueller matrix be block diagonal, the ellipsometric parameters can be determined by only 4 nonzero elements of the Mueller matrix. Thus, the optimal instrument matrix presented by Anna et al. and the relevant configurations determined by Mu et al. could no longer be optimal for the measurement of ellipsometric parameters [28,29]. Li et al. minimized the summation variance of the partial elements in the block diagonal Mueller matrix by using the method proposed by Anna et al. and demonstrated another ideal instrument matrix model [30]. In applications, it is needed to determine practical MMP

* Corresponding author.
E-mail address: quanncx@hotmail.com (N. Quan).

https://doi.org/10.1016/j.photonics.2018.01.004
1569-4410/

configuration that can generate the ideal instrument matrix for the measurement of block diagonal Mueller matrix used to determine the ellipsometric parameters. However, as far as we know, no such practical configuration has been developed and reported.

In this paper, we address the issue of determining the practical configuration of the MMP for measuring the ellipsometric parameters of anisotropic optical materials with immunity to both Poisson shot noise and additive Gaussian noise. A typical configuration of MMP is optimized by a cost function that accounted for Manhattan distance between the rows of the generated instrument matrices and those of the optimal ones. The performances of our optimized configuration and the existing ones are compared, and the results demonstrate that the configuration proposed in this paper can lead to lower total variance of the Mueller matrix elements related to the ellipsometric parameters.

2. Theory

2.1. Instrument matrix

The linear equation of MMP is

$$\mathrm{V}_I = [A \otimes W]^T \mathrm{V}_M \tag{1}$$

where V_I and V_M are 16 dimensional vectors corresponding to the 16 measurement intensities and 16 elements of the measured Mueller matrix of the sample, respectively. T denotes the transpose of the matrix, $\otimes$ denotes the Kronecker product. The instrument matrices W and A represent 4 Stokes vectors that characterize the different polarization states of the PSG and PSA, respectively. In particular, the polarization states of PSG and PSA are identical, which means $A = W$ [15,17,19]. The instrument matrix A is given by

$$\mathrm{A} = \frac{1}{2}\begin{bmatrix} 1 & A_{11} & A_{12} & A_{13} \\ 1 & A_{21} & A_{22} & A_{23} \\ 1 & A_{31} & A_{32} & A_{33} \\ 1 & A_{41} & A_{42} & A_{43} \end{bmatrix}^T \tag{2}$$

where the first and the second subscripts correspond to ith measurement intensity and jth Stokes parameter generated by PSA or PSG, respectively. The vector of Mueller matrix V_M can be estimated by [15]

$$\mathrm{V}_M = \left[A^{-1} \otimes A^{-1}\right]^T \mathrm{V}_I \tag{3}$$

The noise in each detected intensity is independent from the other statistically, the covariance matrix Γ_{V_I} of the vector V_I is a diagonal matrix, and each diagonal element equals to the variance of each detected intensity [15]. The variance of V_M can be characterized by its covariance matrix Γ_{V_M}

$$\Gamma_{\mathrm{V}_M} = \left[A^{-1} \otimes A^{-1}\right]^T \Gamma_{\mathrm{V}_I} \left[A^{-1} \otimes A^{-1}\right] \tag{4}$$

The ellipsometric parameters of isotropic reflecting surface and some anisotropic thin film samples can be calculated by only four elements that indicated in the following the block diagonal Muller matrix.

$$M = \begin{bmatrix} m_{11} & m_{12} & \bullet & \bullet \\ \bullet & \bullet & \bullet & \bullet \\ \bullet & \bullet & m_{33} & m_{34} \\ \bullet & \bullet & \bullet & \bullet \end{bmatrix} \tag{5}$$

where the symbol "•" refers to the matrix elements irrelevant to the ellipsometric parameters, and σ_i^2 corresponds to the variance of the four elements (m_{11}, m_{12}, m_{33}, m_{34}).

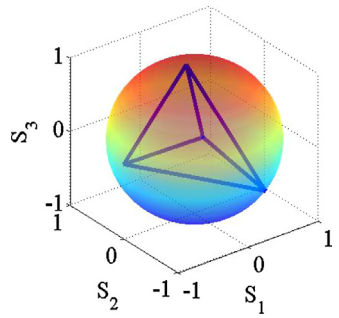

Fig. 1. The last three elements of each row from the 4-elements instrument matrix inscribes a regular tetrahedron with maximum volume inside a Poincaré sphere of unit radius.

The ellipsometric parameters Ψ and Δ of an isotropic reflecting surface or anisotropic optical material can be measured by MMP. Ψ and Δ are defined by the complex Fresnel coefficients r_p and r_s (r_p is the complex Fresnel coefficient parallel to the incident plane and r_s is that perpendicular to the incident plane). $\Psi = \tan^{-1}|r_p/r_s|$ is the amplitude ratio upon reflection, and $\Delta = \delta_p - \delta_s$ is the difference in phase shift. The ellipsometric parameters Ψ and Δ can be obtained from the partial Mueller matrix described in Eq. (5):

$$\Psi = \frac{1}{2}\cos^{-1}\left[\frac{-m_{12}}{m_{11}}\right], \Delta = \tan^{-1}\left[\frac{m_{34}}{m_{33}}\right] \tag{6}$$

To minimize the total variance of the four elements in Mueller matrix, the optimal instrument matrix should satisfy the following relation

$$A = arg\min \sum_{i \in \Omega} \sigma_i^2, \Omega = \{1, 2, 11, 12\} \tag{7}$$

If the dominant noise is Gaussian noise, the covariance matrix Γ_{V_I} is a diagonal matrix with the diagonal elements equal to the variance of Gaussian noise σ^2. The variance of each element of V_M only depend on the instrument matrix A and it is given by

$$\sigma_i^2 = \sigma^2 \left[\left[AA^T\right]^{-1} \otimes \left[AA^T\right]^{-1}\right]_{ii}, \forall i \in \Omega \tag{8}$$

If the dominant noise is Poisson shot noise, the variance of each element of V_M is related to the first element of V_M and it can be expressed by

$$\sigma_i^2 = \frac{[\mathrm{V}_M]_1}{4} \left[\left[AA^T\right]^{-1} \otimes \left[AA^T\right]^{-1}\right]_{ii}, \forall i \in \Omega \tag{9}$$

By using Eq. (7) and Eq. (8), the ideal instrument matrix with the immunity to both Poisson and Gaussian noise can be obtained [30]

$$A^*_{4\text{-}elems} = \frac{1}{2}\begin{bmatrix} 1 & 0.443 & 0.732 & 0.518 \\ 1 & 0.443 & -0.732 & -0.518 \\ 1 & -0.443 & 0.732 & -0.518 \\ 1 & -0.443 & -0732 & 0.518 \end{bmatrix}^T \tag{10}$$

The last three elements in each row of the ideal instrument matrix are coordinates of eigenvectors of the MMP system. These normalized vectors consist a tetrahedron inside a Poincaré sphere of unit radius, which is shown in Fig. 1. It can be seen that the tetrahedron are regular, which means the configurations described by the instrument matrix of Eq. (10) are optimized and have the best noise immunity to the Poisson shot noise and Gaussian noise [31–33]. However, the existing practical configurations cannot generate the ideal measurement matrix so far.

Table 1
Optimized retardations and azimuths of retarders of MMP configurations for the measurement of 4-elements Mueller matrix.

Parameter/deg	Cost function Eq. (11)	Cost function Eq. (13)
(Retardance, Azimuth)	(121.20, 71.34) (121.20, −71.34) (144.48, 31.56) (144.48, −31.56)	(120.04, 72.05) (120.04, −72.05) (143.27, −32.12) (143.27,32.12)

2.2. Cost function

In this paper, we build a cost function that similar to Ref. [27] by considering the last three columns of $A^*_{4\text{-}elems}$ as figures of merit

$$\left(\theta_i, \delta_i\right) = \underset{\theta,\delta}{arg\,min} \sqrt{\sum_{j=1}^{3} |A_{i,j}\left(\theta, \delta\right) - A^*_{4\text{-}elems\,i,j}|} \tag{11}$$

The cost function is used to account for the Manhattan distance between the rows of the instrument matrix and those of the ideal matrix. Since the last three elements $A_{i,j}$ in each row of Eq. (2) the function of the retardation δ and azimuth θ of the retarder, optimal retardation and azimuth to generate the ideal instrument matrix can be obtained with Eq. (10).

3. Optimal configuration

In this section, a typical practical configuration will be optimized by the cost function. Since the instrument matrix of PSG and PSA are identical, we choose the PSA as the configuration to be optimized. It consists of a rotatable retarder with variable retardation δ_i and a variable azimuth θ_i followed by a fixed a horizontal polarizer as shown in Fig. 2. It should be noted that other configurations can be also optimized by the cost function, such as the configuration consists of two rotatable retarders with variable retardances and a fixed polarizer. The PSA consists of variable retarder followed by a fixed polarizer that can make the detector have the same polarization response. The ith row vector of the instrument matrix of the configuration can be given by

$$\mathrm{V}_i = \frac{1}{2}\begin{bmatrix} 1 & \cos^2 2\theta_i + \sin^2 2\theta_i \cos\delta_i & \sin^2 4\theta_i \sin^2\delta_i/2 & -\sin 2\theta_i \sin\delta_i \end{bmatrix} \tag{12}$$

Another cost function has been presented by Mu et al. to determine the optimal configurations of Full-Stokes polarimeter. It is used to account for the Euclidean distance between the rows of the measurement matrix and the rows of the ideal matrix given by [27]:

$$\left(\theta_i, \delta_i\right) = \underset{\theta,\delta}{arg\,min} \sqrt{\sum_{j=1}^{3} |A_{i,j}\left(\theta, \delta\right) - A^*_{4\text{-}elems\,i,j}|^2} \tag{13}$$

Substituting the last three elements of $\mathbf{V}_i$ into the cost functions, the optimal parameters (δ_i, θ_i) can be determined. This procedure is accomplished using code developed in MATLAB software and several candidate parameters can be founded in Fig. 3 and Fig. 4. The optimized parameters (δ_i, θ_i) corresponding to the ideal Mueller matrix $A^*_{4\text{-}elems}$ are shown in Table 1.

In order to compare the optimal configurations obtained by the two cost functions, we consider the measurement perturbed by noises. The variance matrix corresponds to the measured Mueller matrix can be determined by Eq. (8) and Eq. (9) when the measurement perturbed by Gaussian additive noise and Poisson shot noise, respectively. The only difference between Eq. (8) and Eq. (9) is that the constant variance σ^2 is replaced by the first element of the measured Mueller matrix $[\mathrm{V}_M]_1/4$. Noting that the variance matrix obtained by Eq. (8) does not depend on the Mueller matrix to be measured in presence of Gaussian additive noise, which means that the optimal configurations have the same performance for different Mueller matrices. Variances of Mueller matrix elements obtained by the configurations optimized by the two cost functions are shown in Table 2. It can be seen that the total variance of the four elements corresponding to the ideal instrument matrix optimized by the two cost functions are both very close to the ideal value of 16.5, while the instrument matrix of the practical configuration obtained by the cost function proposed in this work corresponds to the minimum total variance. Compare with the configuration obtained by cost function of Eq. (13), the total variance of these four elements are decreased by 1.2%.

It should be declared that the tiny reduction appeared in the total variance of the reconstructed Mueller matrix by using the cost function in Eq. (11) cannot serve as evidence to indicate that one optimal configuration is preferable to another. The retardations and azimuths obtained by the two methods are very close to each other. The last three elements on each row of the instrument matrices correspond to the configurations obtained by the cost functions all inscribe a regular tetrahedron with maximum volume in a Poincaré sphere of unit radius, which are shown in Fig. 5. In other words, the optimized configurations both have the best noise immunity to the Poisson shot noise and Gaussian noise.

Table 3
The reported optimized retardances and azimuths of retarders for the PSG/PSA configurations.

Configuration	Retardance/deg	Azimuth/deg
Config.I	(121.20, 148.8)	(±71.34, ±31.56)
Ref. [31]	90	(−45,0.30,60)
Ref. [19]	90	PSA: (−50.56, −14.80,14.80,50.56) PSG: (−101.51, −72.1, −36.99,41.44)
Ref. [18]	132	(±15.1, ±51.7)
Ref. [27]	(102.2, 142.1)	(±71.9, ±34.95)

4. Performance comparison

Two types of existing configuration are chosen to demonstrate the advantage of the optimized configuration in Section 3. One is obtained by minimizing the condition number (CN) of the instrument matrix [19,31]. The other is presented by minimizing the Euclidean length of the row of the inverse instrument matrix, named equally weighted variance (EWV) [18,27]. The practical configurations are listed in Table 3 and Config.I denotes the con-

Table 2
Variance of each element in Mueller matrix for instrument matrices optimized by the two cost functions in the presence of noises. The total variance of the four Mueller elements is also presented.

Var[M]	Cost function Eq. (13)	Cost function Eq. (11)
$\sigma^2/\frac{[\mathrm{V}_M]_1}{4}$	$\begin{bmatrix} 1.008 & 4.441 & 2.000 & 3.649 \\ 4.441 & 19.710 & 8.876 & 16.193 \\ 2.000 & 8.876 & 3.997 & 7.792 \\ 3.649 & 16.193 & 7.292 & 13.304 \end{bmatrix}$	$\begin{bmatrix} 1.000 & 5.105 & 1.867 & 3.721 \\ 5.105 & 26.056 & 9.532 & 18.995 \\ 1.867 & 9.532 & 3.487 & 6.948 \\ 3.721 & 18.995 & 6.948 & 13.847 \end{bmatrix}$
Total variance	16.738	16.540

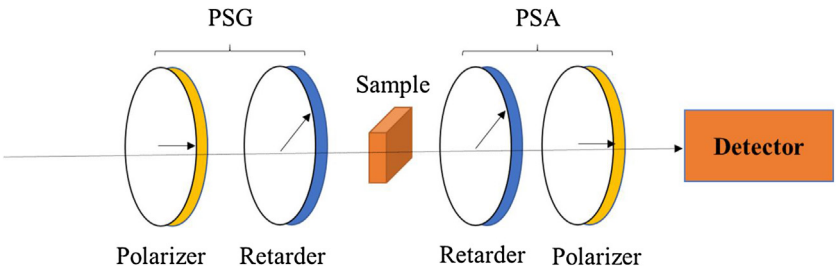

Fig. 2. Configuration of MMP consist of a variable retarder and a horizontal polarizer.

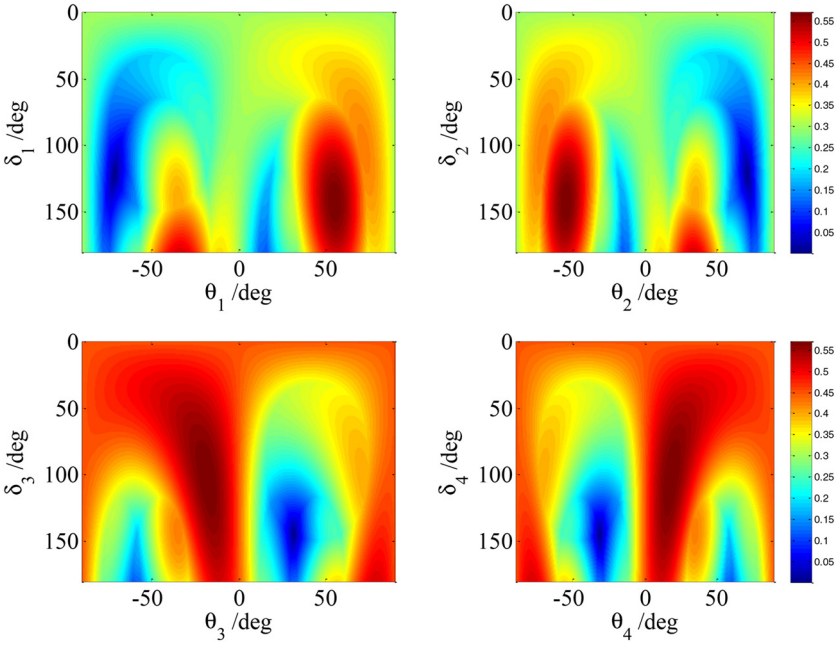

Fig. 3. The value of cost function in Eq. (11) varies with the retardance δ_i and azimuth θ_i for the configuration with a retarder corresponding to matrix $A^*_{4\text{-}elems}$.

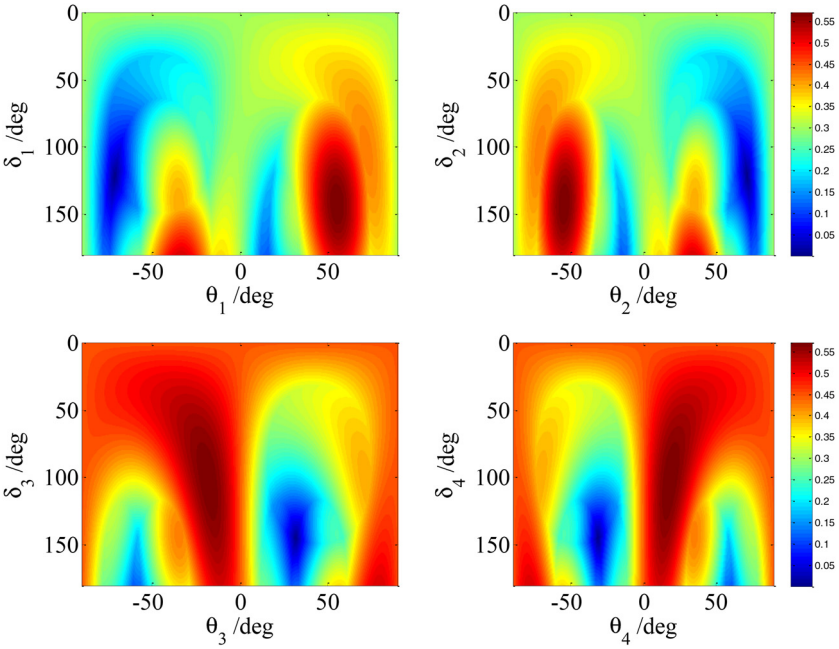

Fig. 4. The value of cost function in Eq. (13) varies with the retardance δ_i and azimuth θ_i for the configuration with a retarder corresponding to matrix $A^*_{4\text{-}elems}$.

Table 4
The total variance of the eight Mueller elements obtained by different practical configurations and the ratio of optimization (ROP) are also presented.

Configuration	Ref. [31]	Ref. [27]	Ref. [19]	Ref. [18]	Config.I
Total variance	150.770	21.94	34.523	21.986	16.540
ROP	89.02%	24.61%	52.09%	24.77%	

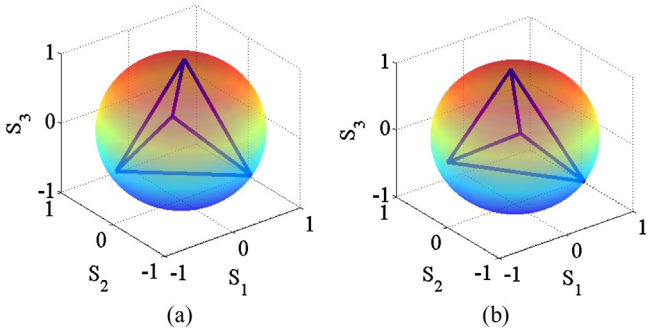

Fig. 5. The last three elements of each row from the instrument measurement matrix inscribe a regular tetrahedron with maximum volume inside a Poincaré sphere of unit radius (a) cost function in Eq. (11) (b) cost function in Eq. (13).

figuration obtained by the cost function in Eq. (11) for the four elements measurement. It should be noted that the variances of estimator correspond to Config.I does not depend on the ellipsometric parameters to be measured, while the variances correspond to other configurations listed in Table 2 depend on the ellipsometric parameters of the sample. Since all possible measured Mueller matrices can be generated by varying Ψ and Δ from 0°to 180°, the minimum total variances of the four elements for these configurations can be determined. Table 4 shows the total variances of the four Mueller matrix elements obtained by the existing configurations. It can be seen that Config.I corresponds to the minimum total variance. Compare with the configurations in Ref. [31] and Ref. [19], a reduction of variance by at least 89.2% and 52.09% can be achieved, respectively. These results demonstrate the configuration proposed in this work can lead to a lower estimation variance of the partial Mueller elements related to the ellipsometric parameters, and thus the estimation precision is considerably improved.

5. Conclusion

In summary, the optimal configuration of Mueller matrix polarimeter for measuring the ellipsometric parameters in the presence of additive Gaussian noise and signal-dependent shot noise is presented. The configuration is optimized by a cost function that accounted for Manhattan distance between the rows of the instrument matrix and those of the ideal matrix. The last three elements on each row of the instrument matrices correspond to the optimized configuration inscribe a regular tetrahedron with maximum volume in a Poincaré sphere of unit radius. The practical configuration can be composed by a 121.2° retardation with a pair of azimuths ±71.34° and a 144.48° retardation with a pair of azimuths ±31.56° for the four Mueller elements measurement. Compared with the existing configurations, the configuration presented in this paper effectively decreases the measurement variance and thus statistically improve the measurement precision of the ellipsometric parameters. The configuration proposed in this work filled some gaps in the field of minimizing the estimation variance for partial Mueller matrix polarimeter. The method of the work can also apply to obtain any optimal configuration of MMP, not limited to the measurement of block diagonal Mueller elements discussed in this paper.

Acknowledgements

The authors thank the anonymous reviewers for their helpful comments and constructive suggestions. The work was supported by the scientific research support program for new teacher of Xi'an University of technology (101-256081706) and National Natural Science Foundation (61275184) of China.

References

[1] R.M. Azzam, N.M. Bashara, Ellipsometry and Polarized Light, Elsevier Science Publishing, 1987.
[2] D. Goldstein, Polarized Light, Dekker, 2003.
[3] H. Tompkins, E. Irene, Handbook of Ellipsometry, William Andrew, 2005.
[4] E. Garcia-Caurel, A. De Martino, J.P. Gaston, L. Yan, Application of spectroscopic ellipsometry and Mueller ellipsometry to optical characterization, Appl. Spectrosc. 67 (2013) 1–21.
[5] K. Hinrichs, K.J. Eichhorn, Ellipsometry of Functional Organic Surfaces and Films, Springer, 2014.
[6] D. Schmidt, A.C. Kjerstad, T. Hofmann, R. Skomski, E. Schubert, M. Schubert, Optical, structural, and magnetic properties of cobalt nanostructure thin films, J. Appl. Phys. 105 (2009) 113508–113519.
[7] T. Oates, H. Wormeester, H. Arwin, Characterization of plasmonic effects in thin films and metamaterials using spectroscopic ellipsometry, Prog. Surf. Sci. 86 (2011) 328–376.
[8] T. Germer, Measurement of roughness of two interfaces of a dielectric film by scattering ellipsometry, Phys. Rev. Lett. 85 (2000) 349–352.
[9] E. Compain, B. Drevillon, Complete high-frequency measurement of Mueller matrices based on a new coupled-phase modulator, Rev. Sci. Instrum. 68 (1997) 2671–2682.
[10] O. Arteaga, J. Freudenthal, B. Wang, B. Kahr, Mueller matrix polarimetry with four photoelastic modulators: theory and calibration, Appl. Opt. 51 (2012) 6805–6817.
[11] G.E. Jellison, F.A. Modine, Two-channel polarization modulation ellipsometer, Appl. Opt. 29 (1990) 959–974.
[12] E. Garcia-Caurel, A.D. Martino, B. Drevillon, Spectroscopic Mueller polarimeter based on liquid crystal devices, Thin Solid Films 455 (2004) 120–123.
[13] L. Aas, P. Ellingsen, M. Kildemo, Near infra-red Mueller matrix imaging system and application to retardance imaging of strain, Thin Solid Films 519 (2010) 2737–2741.
[14] X. Li, T. Liu, B. Huang, Z. Song, H. Hu, Optimal distribution of integration time for intensity measurements in Stokes polarimetry, Opt. Express 21 (2015) 27690–27699.
[15] G. Anna, F. Goudail, Optimal Mueller matrix estimation in the presence of Poisson shot noise, Opt. Express 19 (2012) 21331–21340.
[16] K.M. Twietmeyer, R.A. Chipman, Optimization of Mueller matrix polarimeters in the presence of error sources, Opt. Express 16 (2008) 11589–11603.
[17] X. Li, H. Hu, T. Liu, B. Huang, Z. Song, Optimal distribution of integration time for intensity measurements in degree of linear polarization polarimetry, Opt. Express 7 (2016) 7191–7200.
[18] S.E. Frantz, K. Morten, S.N. Ingar, L. Mikeal, Well-conditioned multiple laser Mueller matrix ellipsometer, Opt. Eng. 47 (2008) 073604.
[19] J.V. Isreal, G.H. Brian, Noise reduction in a laser polarimeter based on discrete waveplate rotations, Opt. Express 16 (2008) 11589–11603.
[20] F. Liu, C.J. Lee, J. Chen, E. Louis, P.J.M. van der Slot, K.J. Boller, F. Bijkerk, Ellipsometry with randomly varying polarization states, Opt. Express 20 (2012) 870–878.
[21] H. Hu, E. Garcia-Caurel, G. Anna, F. Goudail, Simplified calibration procedure for Mueller polarimeter in transmission configuration, Opt. Lett. 39 (2014) 418–421.
[22] A. De Martino, Y.K. Kim, E. Garcia-Caurel, B. Laude, B. Drévillon, Optimized Mueller polarimeter with liquid crystals, Opt. Lett. 28 (2003) 616–618.
[23] S. Krishnan, P.C. Nordine, Mueller-matrix ellipsometry using the division-of-amplitude photopolarimeter: a study of depolarization effects, Appl. Opt. 33 (1994) 4184–4192.
[24] S.N. Savenkov, Optimization and structuring of the instrument matrix for polarimetric measurements, Opt. Eng. 41 (2002) 965–972.
[25] H. Hu, R. Ossikovski, F. Goudail, Performance of Maximum Likelihood estimation of Mueller matrices taking into account physical realizability and Gaussian or Poisson noise statistics, Opt. Express 21 (2013) 5117–5129.
[26] J.S. Tyo, Z. Wang, S.J. Johnson, B.G. Hoover, Design and optimization of partial Mueller matrix polarimeters, Appl. Opt. 49 (2010) 2326–2333.
[27] T. Mu, Z. Chen, C. Zhang, R. Liang, Optimal configurations of full-Stokes polarimeter with immunity to both Poisson and Gaussian noise, J. Opt. 18 (2016) 055702.
[28] E. Compain, S. Poirier, B. Drevillon, General and self-consistent method for the calibration of polarization modulators, polarimeters, and mueller-matrix ellipsometers, Appl. Opt. 38 (1999) 3490–3502.
[29] S.B. Hatit, M. Foldyna, A. De Martino, B. Drevillon, Angle-resolved Mueller polarimeter using a micro- scope objective, Phys. Stat. Sol. (a) 205 (2008) 743–747.

[30] X. Li, H. Hu, L. Wu, T. Liu, Optimization of instrument matrix for Mueller matrix ellipsometry based on partial elements analysis of the Mueller matrix, Opt. Express 25 (2017) 18872–18885.
[31] A. Ambirajan, D.C. Look, Optimum angles for a polarimeter: I, Opt. Eng. 34 (1995) 1651–1655.
[32] T. Mu, C. Zhang, R. Liang, Demonstration of a snapshot full-Stokes division-of aperture imaging polarimeter using Wollaston prism array, J. Opt. 17 (2015) 125708.
[33] D.S. Sabatke, M.R. Descour, E.L. Dereniak, W.C. Sweatt, S.A. Kemme, G.S. Phipps, Optimization of retardance for a complete Stokes polarimeter, Opt. Lett. 25 (2000) 802–804.